Supporting Information

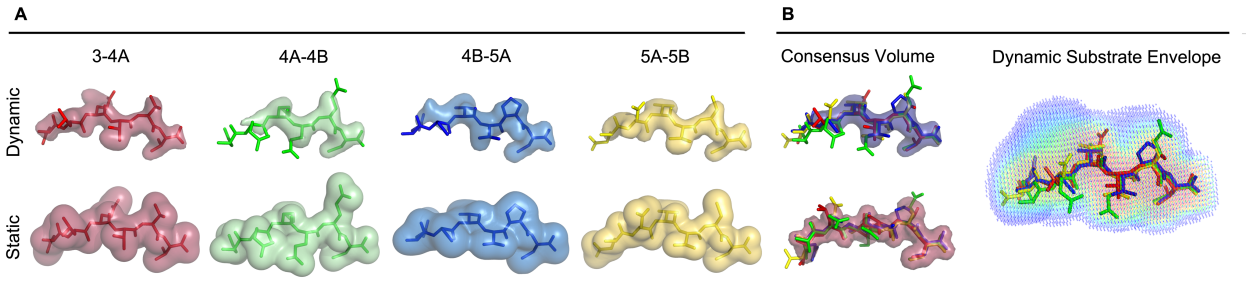

Figure S1. (A) Substrate flexibility reduces the consensus volume as reflected in dynamic volumes smaller than static substrate volumes. The vdW volume occupied by 75% of substrate conformers during MD simulations (*Dynamic*) is compared to the vdW volume of the crystal structure conformation (*Static*) for substrates 3-4A, 4A-4B, 4B-5A, 5A-5B. (B) Dynamic substrate envelope is a more realistic representation of the conserved substrate volume. The dynamic consensus volume is the volume occupied by at least 75% of substrate conformers in the MD simulation trajectories, whereas the static consensus volume is the volume occupied by at least 3 of 4 substrates in the crystal structures. The *dynamic substrate envelope* is the probability distribution of vdW volume occupied by all substrate conformers in the MD simulations. Substrate co-crystal structures in stick representation are superposed (P6 to P1 orientation left to right) onto the grid matrix of the dynamic substrate envelope. Panel A and the consensus volumes in Panel B were visualized in PyMOL by loading the substrate conformations from pre-aligned snapshots of MD simulations. A vdW map was generated for each conformer using the *map_new* functionality. The maps were then summed using the *map_set* function. The final map was shown in surface representation with a contour level that corresponds to 25% of the total number of conformations used.

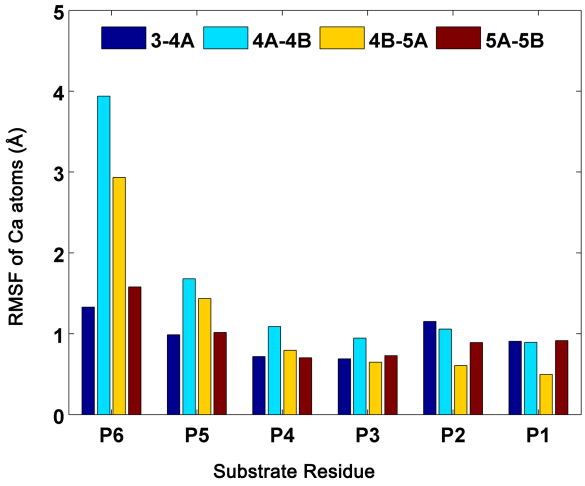

Figure S2. P4-P1 substrate region is less mobile compared to P6 and P5 residues, contributing to the highly conserved consensus volume. The root-mean-squared-fluctuations (RMSF) of Ca atoms of each substrate were calculated from MD simulations. The relatively high mobility of 4A-4B likely causes the substrate to sample a wider conformational space, resulting in a smaller dynamic volume (Figure S1).

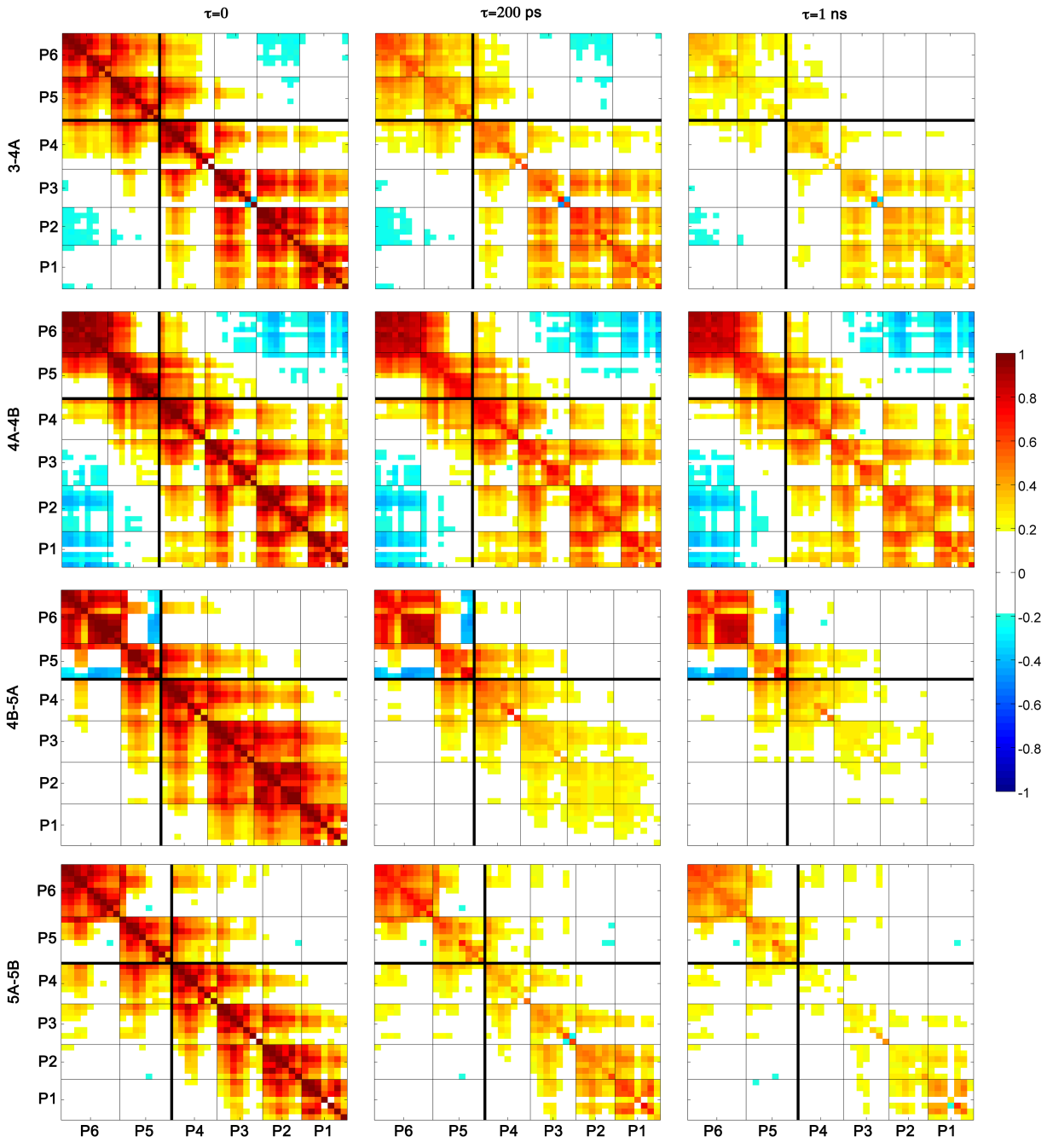

Figure S3. Correlation of substrate atomic fluctuations within P4-P1 region survives longer compared to those across P6-P5 and P4-P1. Residues are separated by lines, the P6-P5 and P4-P1 regions are separated by a thicker black line.

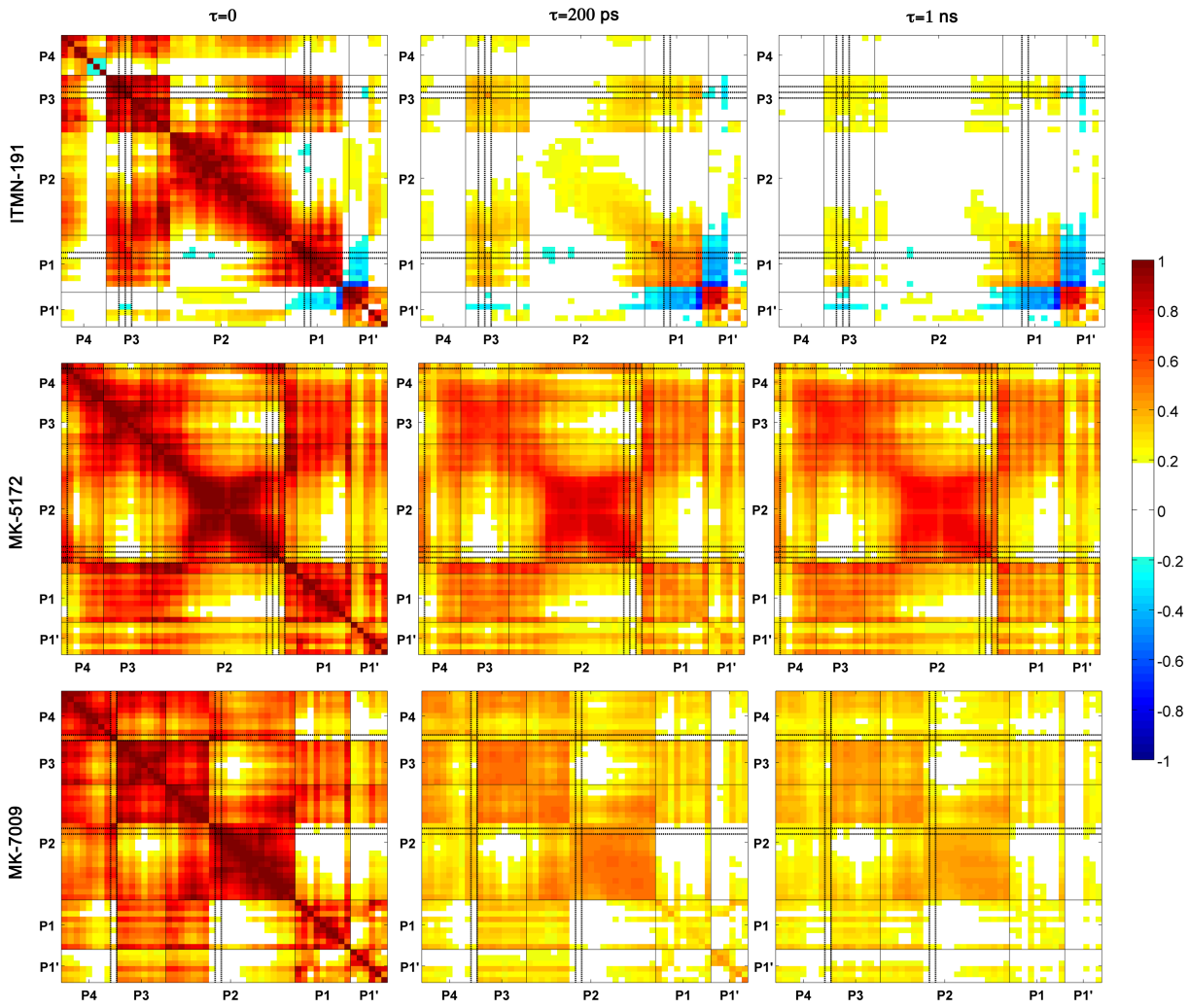

Figure S4. Inhibitor atomic fluctuations are highly correlated and correlations survive longer in compounds with P2-P4 macrocycle (MK-5172 and MK-7009). Residues are separated by lines, and the macrocyle linker atoms are indicated by darker lines.

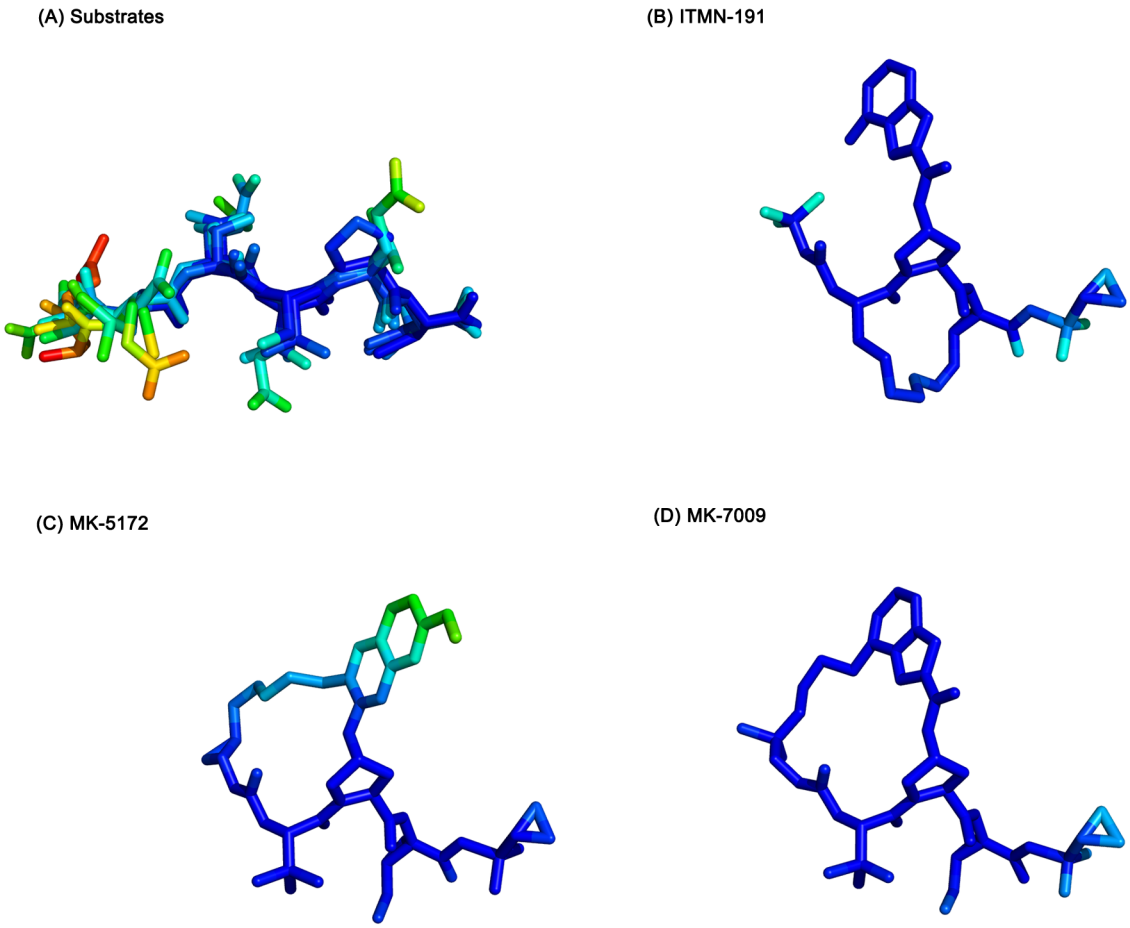

Figure S5. Compound flexibility is dictated by a combination of features (status/location of the macrocycle, connection points of the linker, and identity of the P2 moiety connected by the linker). The RMSF of substrate and inhibitor atoms are mapped onto the structures of (A) four substrates, (B) ITMN-191, (C) MK-5172, and (D) MK-7009. Warm colors indicate more flexible regions and cool colors correspond to rigid regions.

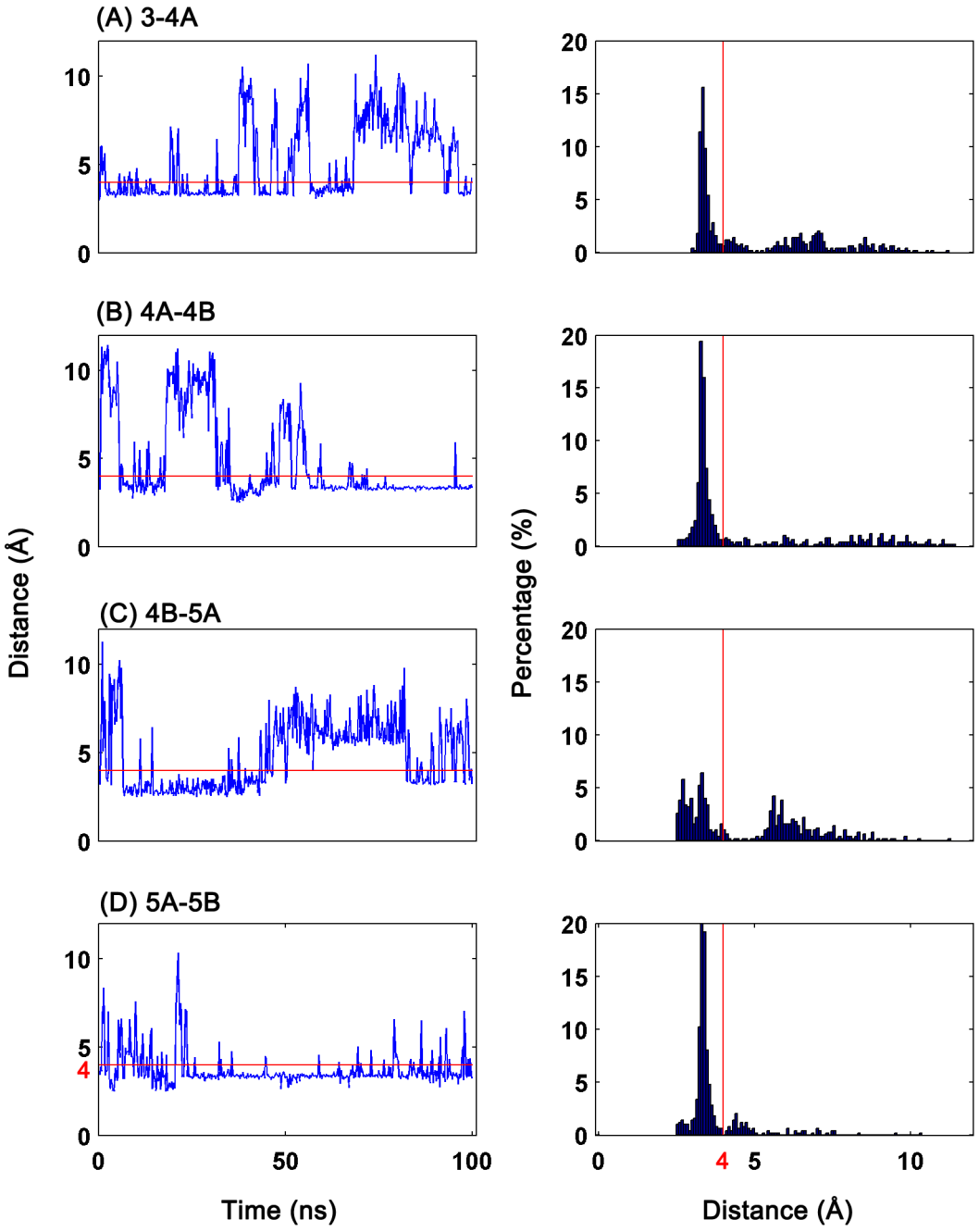

Figure S6. P6 Asp/Glu of substrates participates in a dynamic salt bridge network with the protease residues R119, R123, R161 and K165. The salt bridge distance over simulation time (left) and the corresponding histogram (right) is displayed for (A) 3-4A, (B) 4A-4B, (C) 4B-5A, and (D) 5A-5B. Salt bridges were defined as an interaction between a side-chain oxygen atom of

Asp or Glu within 4.0 Å of a nitrogen atom of Arg or Lys (indicated by the red horizontal and vertical lines).

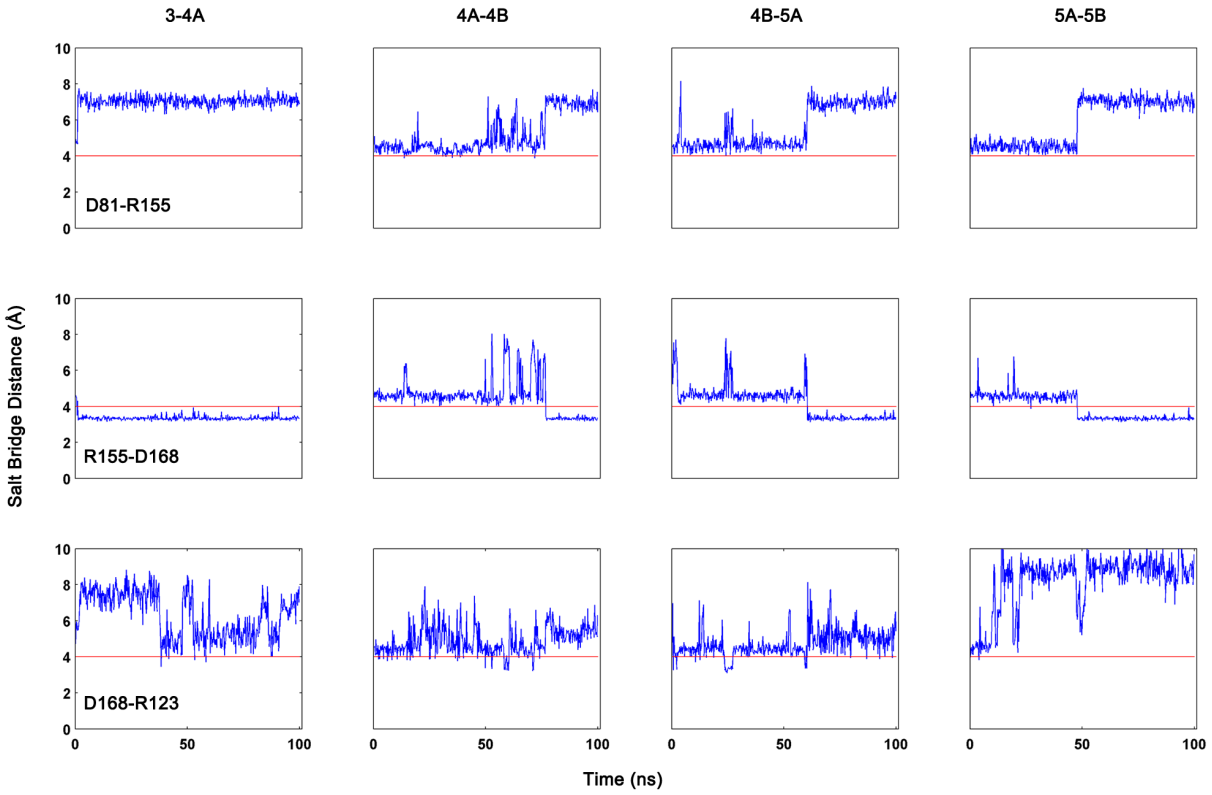

Figure S7. R155 is shared by D81 and D168 in a salt bridge network along the binding surface. The salt bridges formed along the binding surface by three pairs of protease residues (D81-R155, R155-D168, and D168-R123) were monitored throughout the 100 ns MD simulation trajectory for four substrate complexes (3-4A, 4A-4B, 4B-5A, 5A-5B).

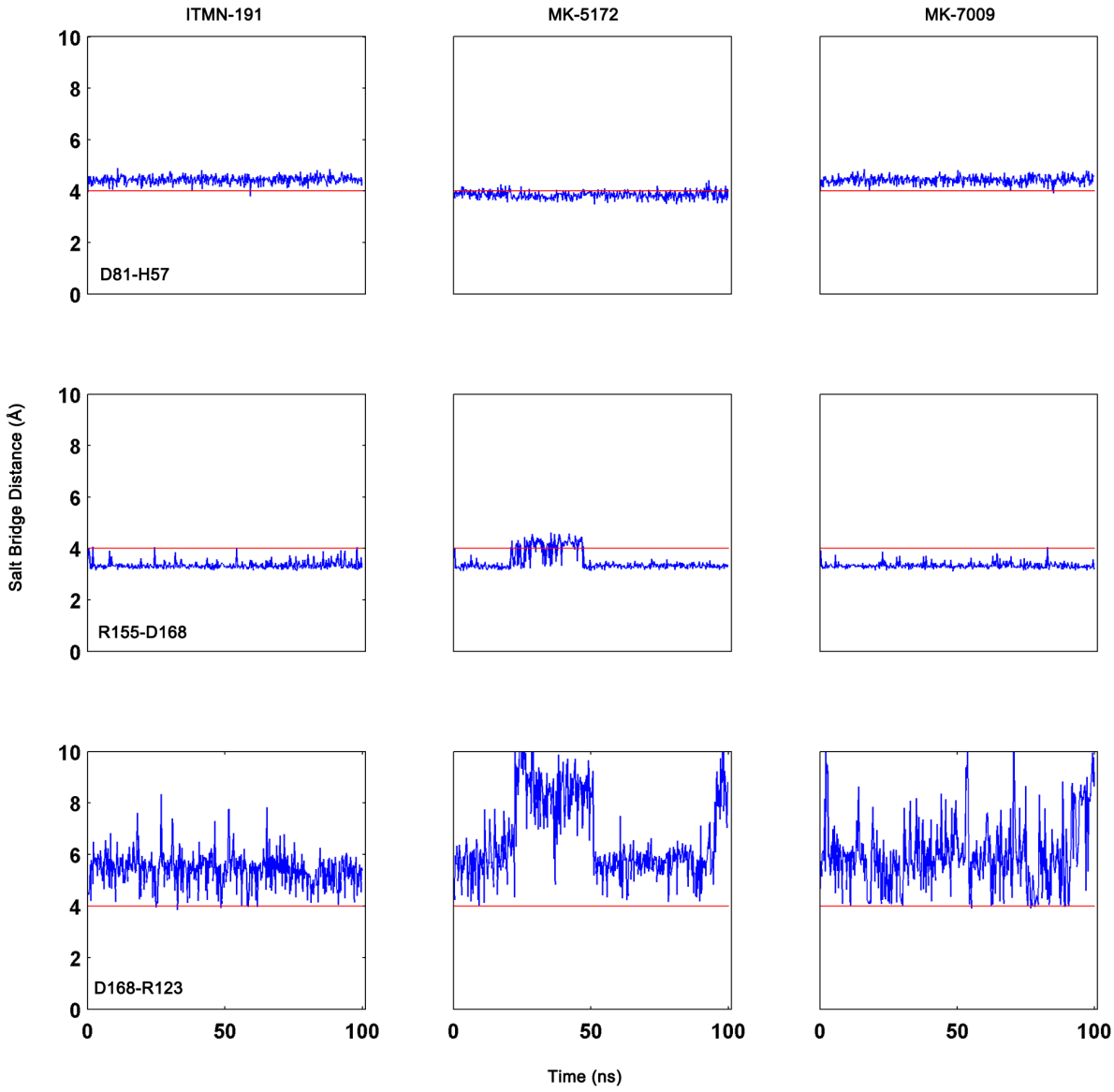

Figure S8. The R155-D168 salt bridge is stabilized by D81-H57 salt bridge in inhibitor complexes. The salt bridges formed along the binding surface by three pairs of protease residues (D81-H57, R155-D168, and D168-R123) were monitored throughout the 100 ns MD simulation for three inhibitor complexes (ITMN-191, MK-5172, and MK-7009).